Active-Site Revealed for Water Oxidation on Electrochemically Induced δ-MnO_2: Role of Spinel-to-layer Phase Transition

Ye-Fei Li* and Zhi-Pan Liu*

Collaborative Innovation Center of Chemistry for Energy Material, Key Laboratory of Computational Physical Science (Ministry of Education), Shanghai Key Laboratory of Molecular Catalysis and Innovative Materials, Department of Chemistry, Fudan University, Shanghai 200433, China

1. Details for SSW Reaction Pathway Sampling

First, we determine the relevant ions/molecules that may trigger the spinel-to-layer phase transition. These ions/molecules should satisfy at least two criteria in thermodynamics: (i) The addition of them should stabilize spinel phase compared to the pristine Mn_3O_4 spinel in OER condition (voltage > 1.23V), and (ii) the spinel-to-layer phase transition is thermodynamically favored ($\Delta G<0$). The possibility of water molecules insertion into spinel frameworks of MnO_2 is first examined, which is found to be thermodynamically unfavorable (>1eV per water) due to the strong repulsion between H_2O and lattice O (too small cage with radius of ~2.0Å in the spinel lattice). This indicates the insertion of water into spinel bulk cannot occur before the phase transition. Furthermore, by examining the spinel and layer structures for a set of crystal phases, including Mn_3O_4, Mn_5O_8, MnO_2, $H_{0.5}MnO_2$, $Li_{0.5}MnO_2$ and $Mg_{0.5}MnO_2$, as listed in Table 1, we found that only for $H_{0.5}MnO_2$ and MnO_2 phases, the layer structure is more stable than their spinel counterpart. For Mn_3O_4, Mn_5O_8, $Li_{0.5}MnO_2$, and $Mg_{0.5}MnO_2$, the spinel phase is at least 0.13 eV/f.u. more stable than the layer phase. These preliminary energetics screening suggests that the hydrogenated-MnO_2 and MnO_2 are the most likely precursor phase for the spinel-to-layer transition.

Table 1. Reaction energy ΔE for the spinel-to-layer transition for different MnO_x-based phases.

Component	ΔE*	Component	ΔE
$H_{0.5}MnO_2$	-0.03	Mn_5O_8	+0.13
MnO_2	-0.06	$Li_{0.5}MnO_2$	+0.17
Mn_3O_4	+0.49	$Mg_{0.5}MnO_2$	+0.35

*$\Delta E = E_{layer} - E_{spinel}$ (eV per Mn f.u.).

Second, we choose MnO_2, $H_{0.5}MnO_2$ and $Li_{0.5}MnO_2$ as the initial state (IS) for SSW pathway sampling to identify the spinel-to-layer pathways. Our test SSW-RS calculations show that $Li_{0.5}MnO_2$ as the IS can visit frequently the spinel-to-layer phase transition pathways, while the proton shifting reactions due to their low barriers are much preferable in the pathway sampling of $H_{0.5}MnO_2$ and no spinel-to-layer pathway was found in the pathway sampling of MnO_2 This agrees with the fact that Mn^{4+} is difficult to migrate within MnO_2 framework as observed in experiment.[1] Therefore, starting from $Li_{0.5}MnO_2$, 20 SSW-RS jobs for each phase were run massively parallel. With 2000 SSW sampling steps, 320 pathways were collected, from which 10 low energy pathways with barrier lower than 0.7 eV/f.u. were identified.

Third, we replace Li with proton in the located four lowest energy pathways and by considering all the likely proton positions (proton adsorbs at the lattice O), we refine all the reaction pathways using the VC-DESW method. All located TSs have been confirmed by extrapolating the TS towards the IS and FS and also the numerical vibrational frequency analysis.

2. Calculation Details for Theoretical Overpotential

To calculate the OER overpotential, we use the Standard Hydrogen Electrode (SHE: $H^+ + e^- \rightarrow {}^1/_2H_2$, pH = 0, p = 1 bar, T = 298.15K) as reference, where we get

$$\Delta G^o_{SHE} = {}^1/_2 G^o[H_2] - G^o[H^+] - G^o[e^-] = 0 \quad (1)$$

$$G^o[H^+] = {}^1/_2 G^o[H_2] - G^o[e^-] = {}^1/_2 G^o[H_2] + \Phi_w \quad (2)$$

where $G^o[H_2]$, $G^o[H^+]$ are the Gibbs free energy change of H_2 and H^+ in standard condition, while Φ_w is the work function of Pt electrode in SHE. For other pH, the free energy $G[H^+]$ can be calculated as

$$G[H^+] = G^o[H^+] - 0.059\text{pH} \quad (3)$$

Using Eq. 2-3, we can derive the ΔG of an electrochemical half-reaction as described by formula 4.

$$H_nA \rightarrow A + nH^+ + ne^- \quad (4)$$

The ΔG is written as

$$\Delta G = G[A] + nG[H^+] + nG[e^-] - G[H_nA] \quad (5)$$

Substituting Eq. 3 into Eq. 4, we get

$$\begin{aligned}\Delta G &= G[A] + n({}^1/_2 G^o[H_2] - G[e^-]_{SHE} - 0.059\text{pH}) + nG[e^-] - G[H_nA] \\ &= G[A] + {}^n/_2 G^o[H_2] - {}^n/_2 \times 0.059\text{pH} + n(G[e^-] + \Phi_w) - G[H_nA] \\ &= G[A] + {}^n/_2 G^o[H_2] - G[H_nA] + n|e|U - {}^n/_2 \times 0.059\text{pH} \quad (5)\end{aligned}$$

Setting $\Delta G = 0$, the parameter U then is the electrochemical potential for half-reaction of $H_nA \rightarrow A + nH^+ + ne^-$. The calculated overpotential (η) then be calculated by Eq. 6.

$$\eta = U - 1.23 \quad (6)$$

3. Calculation Details for Phase Diagram of Mn_3O_4, H_nMnO_2 and MnO_2

The phase diagram of Mn_3O_4, $H_{0.5}MnO_2$ and MnO_2 involves three consecutive reactions from spinel Mn_3O_4 to $H_{0.5}MnO_2$ and to MnO_2 following the chemical formula below.

$$2Mn_3O_4 + 4H_2O \rightarrow 6H_{0.5}MnO_2 + 5H^+ + 5e^- \quad (7)$$

$$4H_{0.5}MnO_2 \rightarrow 4H_{0.25}MnO_2 + H^+ + e^- \quad (8)$$

$$4H_{0.25}MnO_2 \rightarrow 4MnO_2 + H^+ + e^- \quad (9)$$

Using Mn_3O_4 phase as energy zero point, we rewrite the Eq. 7-9 as

$$Mn_3O_4 + 2H_2O \rightarrow 3H_{0.5}MnO_2 + {}^5/_2 H^+ + {}^5/_2 e^- \quad (10)$$

$$Mn_3O_4 + 2H_2O \rightarrow 3H_{0.25}MnO_2 + {}^{13}/_3 H^+ + {}^{13}/_3 e^- \quad (11)$$

$$Mn_3O_4 + 2H_2O \rightarrow 3MnO_2 + 4H^+ + 4e^- \quad (12)$$

Using SHE as reference (see Section 2 of SI), free energy change in reactions 10-12 can be calculated by following formula.

$$\Delta G[H_{0.5}MnO_2] = 3G[H_{0.5}MnO_2] + {}^5/_4 G[H_2] - G[Mn_3O_4] - 2G[H_2O] - {}^5/_2 |e|U \quad (13)$$

$$\Delta G[H_{0.25}MnO_2] = 3G[H_{0.25}MnO_2] + {}^{13}/_6 G[H_2] - G[Mn_3O_4] - 2G[H_2O] - {}^{13}/_3 |e|U \quad (14)$$

$$\Delta G[MnO_2] = 3G[MnO_2] + 2G[H_2] - G[Mn_3O_4] - 2G[H_2O] - 4|e|U \quad (15)$$

The relative stabilities of H_nMnO_2 and MnO_2 compared with Mn_3O_4 can thus be estimated by Eq. 13-15. By plotting ΔG vs. U, we finally get the phase diagram of Mn_3O_4, H_nMnO_2 and MnO_2. It should be mentioned that the line for Mn_3O_4 is horizontal, since Mn_3O_4 is the reference state where the free energy change is zero for this component.

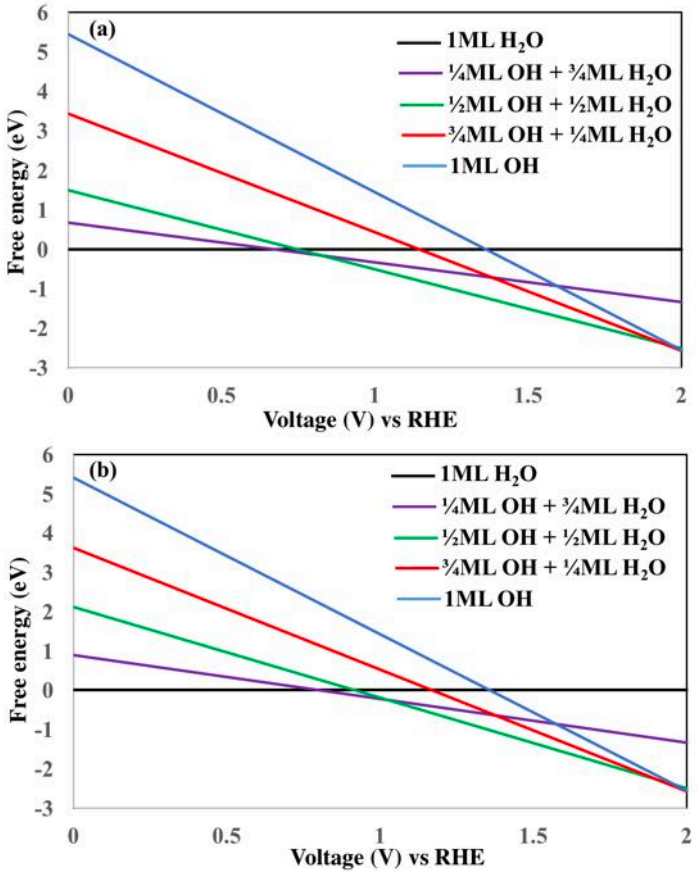

Figure S1. Phase diagram for (a) δ-MnO_2 and (b) pristine spinel Mn_3O_4 in aqueous electrolyte.

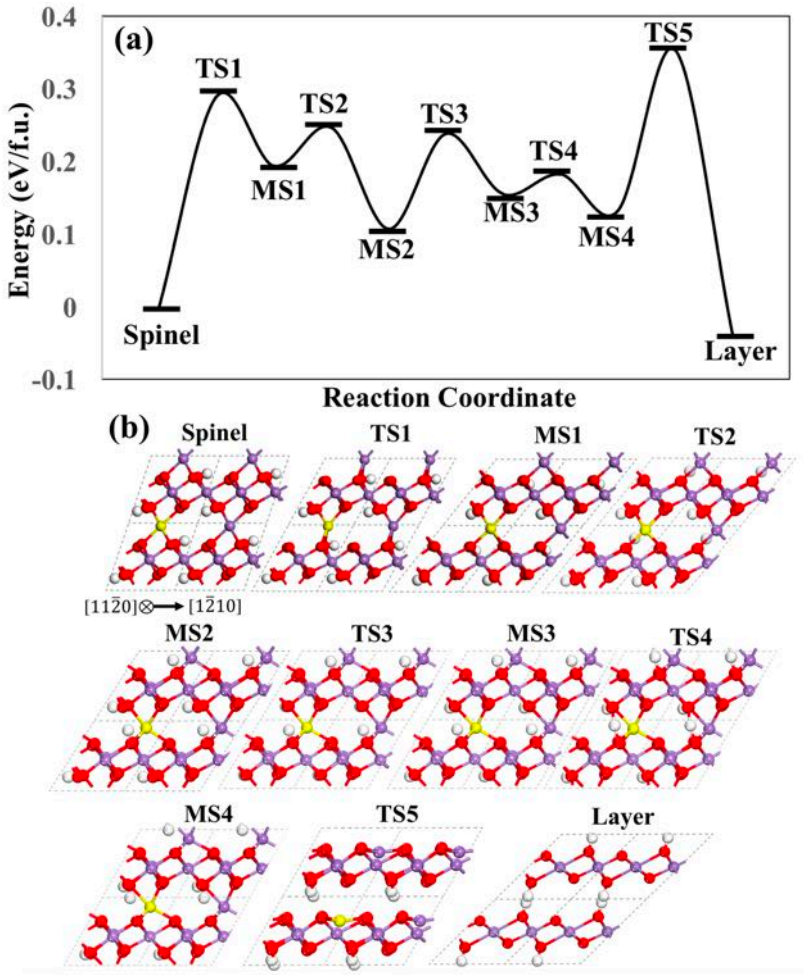

Figure S2. (a) Complete energetic profiles for solid-to-solid phase transition of $H_{0.5}MnO_2$ and MnO_2. (b) Side view of key intermediate states of $H_{0.5}MnO_2$ during phase transition. The dashed boxes are unit cell. The directions are relative to the hexagonal unit cell of δ-MnO_2. It should be mentioned that the Mn atom chains along A site and B site of MnO_2 layers are different. Colors in (c): red ball: O; white ball: H; violet ball: Mn; yellow ball: Mn^{ic}.

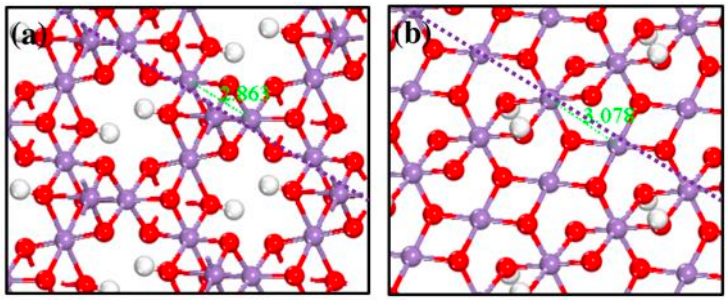

Figure S3. The interfacial strain build in layer-to-spinel transition. (a) spinel (b) layered $H_{0.5}MnO_2$. The dotted lines indicate the $[2\bar{1}\bar{1}0]$ direction, and the green number is the Mn-Mn distance along this direction.

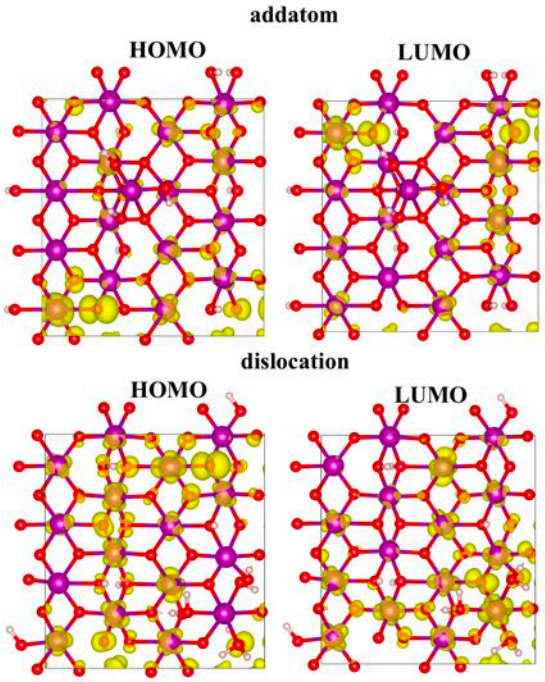

Figure S4. 3D isosurface contour plot for addatom and dislocation structures. The isosurface value is set as 0.0025 $(e/Å^3)^2$.

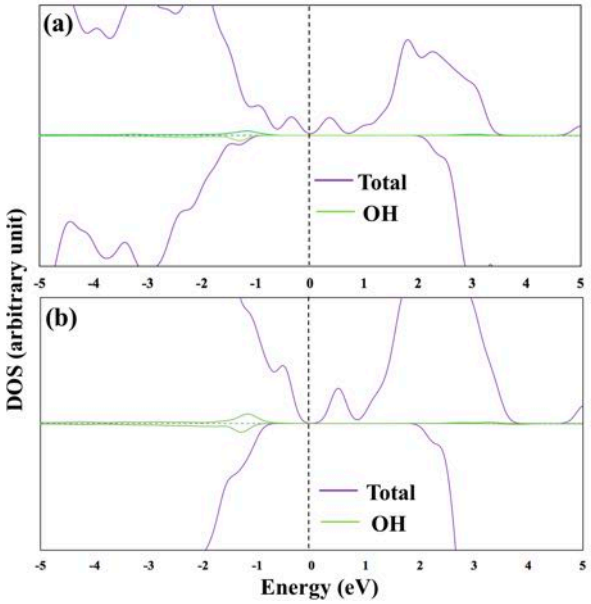

Figure S5. Alignment of energy levels between OH and δ-MnO_2. (a) OH adsorbs on pristine edge and (b) OH adsorbs on edge-NV.

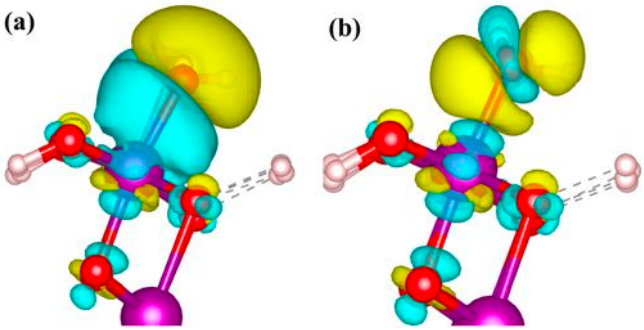

Figure S6. 3D isosurface contour plot of charge density difference for OH adsorption on (a) pristine edge and (b) edge-NV before and after the OH adsorption. The isosurface value is set as 0.0025 $(e/Å^3)^2$. Yellow and Blue density indicate where the charge accumulation and depletion occur, respectively.

References

1. Leifer, N.; Schipper, F.; Erickson, E. M.; Ghanty, C.; Talianker, M.; Grinblat, J.; Julien, C. M.; Markovsky, B.; Aurbach, D., *J. Phys. Chem. C* **2017,** *121*, 9120-9130.